Monthly Notices
of the
ROYAL ASTRONOMICAL SOCIETY

MNRAS **440,** 2610–2615 (2014) doi:10.1093/mnras/stu575

Constraints on the CMB temperature evolution using multiband measurements of the Sunyaev–Zel'dovich effect with the South Pole Telescope

A. Saro,[1,2]★ J. Liu,[1,2] J. J. Mohr,[1,2,3] K. A. Aird,[4] M. L. N. Ashby,[5] M. Bayliss,[5,6] B. A. Benson,[7,8,9] L. E. Bleem,[8,10,11] S. Bocquet,[1,2] M. Brodwin,[12] J. E. Carlstrom,[8,9,10,11,13] C. L. Chang,[8,9,11] I. Chiu,[1,2] H. M. Cho,[14] A. Clocchiatti,[15] T. M. Crawford,[8,13] A. T. Crites,[8,13] T. de Haan,[16] S. Desai,[1,2] J. P. Dietrich,[1,2] M. A. Dobbs,[16] K. Dolag,[1,2] J. P. Dudley,[16] R. J. Foley,[17,18] D. Gangkofner,[1,2] E. M. George,[19] M. D. Gladders,[8,13] A. H. Gonzalez,[20] N. W. Halverson,[21] C. Hennig,[1,2] J. Hlavacek-Larrondo,[22,23] W. L. Holzapfel,[19] J. D. Hrubes,[4] C. Jones,[5] R. Keisler,[8,10] A. T. Lee,[19,24] E. M. Leitch,[8,13] M. Lueker,[19,25] D. Luong-Van,[4] A. Mantz,[8] D. P. Marrone,[26] M. McDonald,[27] J. J. McMahon,[28] J. Mehl,[8,13] S. S. Meyer,[8,9,10,13] L. Mocanu,[8,13] T. E. Montroy,[29] S. S. Murray,[5] D. Nurgaliev,[6] S. Padin,[8,13,25] A. Patej,[6] C. Pryke,[30] C. L. Reichardt,[19] A. Rest,[31] J. Ruel,[6] J. E. Ruhl,[29] B. R. Saliwanchik,[29] J. T. Sayre,[29] K. K. Schaffer,[8,9,32] E. Shirokoff,[19,25] H. G. Spieler,[24] B. Stalder,[5] Z. Staniszewski,[29] A. A. Stark,[5] K. Story,[8,10] A. van Engelen,[16] K. Vanderlinde,[33,34] J. D. Vieira,[17,25] A. Vikhlinin,[5] R. Williamson,[8,13] O. Zahn[19] and A. Zenteno[1,2]

Affiliations are listed at the end of the paper

Accepted 2014 February 19. Received 2014 February 17; in original form 2013 December 7

ABSTRACT

The adiabatic evolution of the temperature of the cosmic microwave background (CMB) is a key prediction of standard cosmology. We study deviations from the expected adiabatic evolution of the CMB temperature of the form $T(z) = T_0(1 + z)^{1-\alpha}$ using measurements of the spectrum of the Sunyaev–Zel'dovich effect with the South Pole Telescope (SPT). We present a method for using the ratio of the Sunyaev–Zel'dovich signal measured at 95 and 150 GHz in the SPT data to constrain the temperature of the CMB. We demonstrate that this approach provides unbiased results using mock observations of clusters from a new set of hydrodynamical simulations. We apply this method to a sample of 158 SPT-selected clusters, spanning the redshift range $0.05 < z < 1.35$, and measure $\alpha = 0.017^{+0.030}_{-0.028}$, consistent with the standard model prediction of $\alpha = 0$. In combination with other published results, we find $\alpha = 0.005 \pm 0.012$, an improvement of ∼10 per cent over published constraints. This measurement also provides a strong constraint on the effective equation of state in models of decaying dark energy $w_{\rm eff} = -0.994 \pm 0.010$.

Key words: galaxies: clusters: general – cosmic background radiation – cosmology: observations – cosmology: theory – submillimetre: general.

1 INTRODUCTION

The existence of the cosmic microwave background (CMB) is a fundamental prediction of the hot big bang theory. The intensity

★ E-mail: saro@usm.lmu.de

spectrum of the CMB radiation locally has been measured by the *COBE* Far Infrared Absolute Spectrophotometer (FIRAS) instrument and found to have a nearly exact blackbody spectrum with a temperature of $T_0 = 2.725\,48 \pm 0.000\,57$ K (Fixsen 2009).

A second fundamental prediction of the hot big bang theory is that the CMB temperature must evolve over cosmic time. Specifically, it is expected to evolve as $T(z) = T_0(1 + z)$ (Tolman 1934), under the assumption that the CMB photon fluid reacts adiabatically to the expansion of the Universe as described by general relativity and electromagnetism. Deviations from the adiabatic evolution of $T(z)$ would imply either a violation of the hypothesis of local position invariance, and therefore of the equivalence principle, or that the number of photons is not conserved. In the former case, this could be associated with variations of dimensionless coupling constants like the fine-structure constant (see, e.g. Martins 2002; Murphy, Webb & Flambaum 2003; Srianand et al. 2004). The latter case is a consequence of many physical processes predicted by non-standard cosmological models, such as decaying vacuum energy density models, coupling between photons and axion-like particles, and modified gravity scenarios (e.g. Matyjasek 1995; Overduin & Cooperstock 1998; Lima, Silva & Viegas 2000; Puy 2004; Jaeckel & Ringwald 2010; Jetzer & Tortora 2011). In all of these models, energy has to be slowly injected or removed from the CMB without distorting the *Planck* spectrum sufficiently to violate constraints from FIRAS (Avgoustidis et al. 2012).

Observational tests of non-standard temperature evolution typically are parametrized by very simple models for the deviation. In particular, we consider here the scaling law proposed by Lima et al. (2000):

$$T(z) = T_0(1 + z)^{1-\alpha}, \quad (1)$$

with α being a free constant parameter.[1] This is the phenomenological parametrization that has been most widely studied by previous authors; deviations of α from zero would result as a consequence of one of the scenarios described above, such as the non-conservation of photon number.

To date, two different observables have been used to determine $T(z)$. At intermediate redshifts ($z \lesssim 1.5$), $T(z)$ can be determined from measurements of the spectrum of the Sunyaev–Zel'dovich effect (SZE; Sunyaev & Zel'dovich 1972), a technique first suggested by Fabbri, Melchiorri & Natale (1978) and Rephaeli (1980). The first attempt to measure $T(z)$ using the spectrum of the SZE was reported in Battistelli et al. (2002) using multifrequency observations of the clusters A2163 and Coma. Luzzi et al. (2009) reported results from the analysis of a sample of 13 clusters with $0.23 \leq z \leq 0.546$. Adopting a flat prior on $\alpha \in [0, 1]$, they provided constraints $\alpha = 0.024^{+0.068}_{-0.024}$, consistent with standard adiabatic evolution.

At high redshift ($z \gtrsim 1$), the CMB temperature can be determined from quasar absorption line spectra which show atomic or molecular fine structure levels excited by the photoabsorption of the CMB radiation. If the system is in thermal equilibrium with the CMB, then the excitation temperature of the energy states gives the temperature of the blackbody radiation (e.g. Srianand, Petitjean & Ledoux 2000; Molaro et al. 2002; Srianand et al. 2008). For example, Noterdaeme et al. (2011) have reported on a sample of five carbon monoxide absorption systems up to $z \sim 3$ where the CMB temperature has been measured. They used their sample, in combination with low-redshift SZE measurements to place constraints on the phenomenological parameter $\alpha = -0.007 \pm 0.027$. This also allowed them to put strong constraints on the effective equation of state of decaying dark energy models $w_{\rm eff} = -0.996 \pm 0.025$. Recently, Avgoustidis et al. (2012) extended this analysis by including constraints inferred from differences between the angular diameter and luminosity distances (the so-called distance-duality relation), which is also affected in models in which photons can be created or destroyed. They also showed that by releasing the positive prior assumption on α the same cluster sample studied in Luzzi et al. (2009) constrains $\alpha = 0.065 \pm 0.080$.

More recently, Muller et al. (2013) fit molecular absorption lines towards quasars to measure the CMB temperature with an accuracy of a few per cent at $z = 0.89$. Combining their data with the data presented in Noterdaeme et al. (2011), they were able to further constrain $\alpha = 0.009 \pm 0.019$.

Constraints on the CMB redshift evolution can be significantly improved by including measurements of the SZE spectrum from experiments, such as the South Pole Telescope (SPT) and *Planck*, with much larger cluster samples. For instance, de Martino et al. (2012) forecast the constraining power of *Planck* to measure α. Using only clusters at $z < 0.3$, they predicted that *Planck* could measure α with an accuracy $\sigma_\alpha = 0.011$. Recently, Hurier et al. (2014) analysed a sample of 1839 galaxy clusters observed with *Planck*. The cluster sample they adopted also included the SPT sample that we analyse here, although it did not contribute significantly to their main results. They were able to constrain $\alpha = 0.009 \pm 0.017$ by stacking the 813 confirmed SZE detected clusters of the *Planck* catalogue (Planck Collaboration 2013) in different redshift bins, with only one cluster in each of their highest redshift bins $z = 0.8$ and $z = 1$. In combination with other available constraints (Luzzi et al. 2009; Noterdaeme et al. 2011; Muller et al. 2013), they limit deviations from adiabatic temperature evolution of the Universe to be $\alpha = 0.006 \pm 0.013$.

In this work, we present constraints on the temperature evolution of the CMB using SZE spectral measurements at the 95 and 150 GHz bands from the SPT. The SPT is a 10 m millimetre-wave telescope operating at the South Pole (Carlstrom et al. 2011) that has recently completed a 2500 deg^2 multifrequency survey of the southern extragalactic sky. Here, we focus on the SZE-selected cluster sample that lies within a 720 deg^2 subregion where optical follow-up and redshift measurements are complete (Song et al. 2012; Reichardt et al. 2013).

2 METHOD

Inverse Compton scattering of the CMB photons by the hot intracluster medium (ICM) induces secondary CMB temperature anisotropies in the direction of clusters of galaxies. Neglecting relativistic corrections, the thermal (tSZE) and kinematic (kSZE) contribution to the temperature anisotropy in the direction $\hat{n}$ of a cluster at a frequency ν can be approximated by (Sunyaev & Zeldovich 1980):

$$\Delta T(\hat{n}, \nu) \simeq T_0(\hat{n})[G(\nu)y_{\rm c}(\hat{n}) - \tau\beta]. \quad (2)$$

Here, $T_0(\hat{n})$ is the current CMB temperature at the direction $\hat{n}$, β is the line-of-sight velocity of the cluster in the CMB frame in units of the speed of light c and τ is the optical depth. The Comptonization parameter $y_{\rm c}$ is related to the integrated pressure along the line of sight $y_{\rm c} = (k_{\rm B}\sigma_{\rm T}/m_{\rm e}c^2)\int n_{\rm e}T_{\rm e}{\rm d}l$ (where $n_{\rm e}$ and $T_{\rm e}$ are, respectively,

[1] In previous literature, this parameter has been referred to with the Greek letter α or β. To avoid confusion with the variable $\beta = v/c$ defined in equation (2), we use α.

the electron density and temperature). In the non-relativistic regime and for adiabatic expansion, $G(x) = x\coth(x/2) - 4$, where the reduced frequency x is given by $x = h\nu(z)/k_{\rm B}T(z) = h\nu_0(1+z)/[k_{\rm B}T_0(1+z)] \equiv x_0$ and is independent of redshift, $\nu(z)$ is the frequency of a CMB photon scattered by the ICM and $T(z)$ is the blackbody temperature of the CMB at the cluster location.

If $T(z) = T_0(1+z)^{1-\alpha}$, then the reduced frequency varies as $x(z, \alpha) = x_0(1+z)^{\alpha}$ and the spectral frequency dependence of $G(\nu)$, the tSZE, now also depends on α: $G(x) = G(\nu_0, \alpha, z)$. From equation (2), neglecting the kSZE contribution, it follows that measuring the ratio of temperature decrements at two different frequencies ν_1 and ν_2 provides

$$R(\nu_1, \nu_2, z, \alpha) \equiv \frac{\Delta T(\hat{n}, \nu_1, z)}{\Delta T(\hat{n}, \nu_2, z)} \simeq \frac{G(\nu_1, z, \alpha)}{G(\nu_2, z, \alpha)}. \quad (3)$$

This ratio is redshift independent for $\alpha = 0$, but not in the case of $\alpha \neq 0$. This method has the advantage that, by taking ratios, the dependence on the Comptonization parameter $y_{\rm c}$ (and therefore on the cluster properties) is removed and the need to account for model uncertainties on the gas density and temperature profile is avoided (Battistelli et al 2002, Luzzi et al 2009). Note that in this approach the distribution of temperature ratios is, in general, non-Gaussian (Luzzi et al. 2009) and needs to be properly modelled.

One important source of noise in these measurements is the primary anisotropy of the CMB. To precisely measure $\Delta T(\hat{n}, \nu)$ for a single cluster, we would have to remove the primary CMB anisotropies in the direction $\hat{n}$. In principle, this could be done by subtracting the CMB temperature measured near the SZE null frequency, which, in the case of $\alpha = 0$ and non-relativistic ICM, is given by a map obtained at 217 GHz (de Martino et al. 2012). Alternatively, because the primary CMB fluctuations are random, it is possible to reduce this source of noise by averaging over a large sample of clusters (e.g. Hurier et al. 2014).

In Reichardt et al. (2013), the SPT cluster sample was selected using a matched multifrequency spatial filter (Melin, Bartlett & Delabrouille 2006), designed to optimally measure the cluster signal given knowledge of the cluster profile and the noise in the maps. The cluster gas profiles are assumed to be well fit by a spherical β model (Cavaliere & Fusco-Femiano 1976), with $\beta = 1$ and 12 possible core radii, θ_c, linearly spaced from 0.25 to 3 arcmin. The noise contributions include, astrophysical (e.g. the CMB, point sources) and the instrumental (e.g. atmospheric, detector) contributions. For each cluster, the maximum signal to noise in the spatially filtered maps was denoted as ξ.

In this work, we measure the ratio of the CMB temperature decrements in the SPT data at 95 and 150 GHz (T_{95} and T_{150}). We extract the cluster signal from the single-frequency spatially filtered maps at 95 and 150 GHz, using the SPT position and core radius favoured by the multifrequency analysis in Reichardt et al. (2013). To compare the decrement at each frequency, we need to account for the smaller beam at 150 GHz. We do this by convolving the 150 GHz data to the same beam size as the 95 GHz noisier data, and then using the 95 GHz filter to extract the signal from the resultant 150 GHz maps. Therefore, we adopt the following Fourier domain spatial filter:

$$\psi(k_x, k_y) = \frac{B_{95}(k_x, k_y)S(|\boldsymbol{k}|)}{B_{95}(k_x, k_y)^2 N_{\rm astro}(|\boldsymbol{k}|) + N_{95}(k_x, k_y)}, \quad (4)$$

where ψ is the matched filter, B_{95} is the SPT beam for the 95 GHz band and S is the assumed source template. The noise contributions $N_{\rm astro}$ and N_{95}, respectively, encapsulate the astrophysical (mainly CMB) and the instrumental noise for the 95 GHz band.

The associated uncertainty ΔT_{95} and ΔT_{150} in the CMB temperature decrement would be equal to the rms of the single-frequency spatially filtered maps. We note that this method is unbiased with respect to the assumed cluster profile. In fact, as the two bands have been homogenized to the larger 95 GHz beam, different assumptions of source template S would only result in tighter or weaker constraints. We also note that, in practice, adopting different cluster profiles as a Gaussian template, Arnaud et al. (2010) or Nagai, Kravtsov & Vikhlinin (2007) pressure profile has a negligible impact on the estimated ξ (Vanderlinde et al. 2010).

Finally, we use the derived values of temperature in the two bands and the associated cluster redshift to constrain α from equation (3) through a maximum likelihood analysis (Luzzi et al. 2009) where the likelihood is defined as

$$\mathcal{L}(\alpha) \propto \prod_{i=1}^{N_{\rm clus}} \exp\left\{ -\frac{[T_{150}^{(i)} R(z^{(i)}, \alpha) - T_{95}^{(i)}]^2}{2[(\Delta T_{150}^{(i)} R(z^{(i)}, \alpha))^2 + (\Delta T_{95}^{(i)})^2]} \right\}, \quad (5)$$

and $R(z, \alpha) \equiv R(95\,{\rm GHz}, 150\,{\rm GHz}, z, \alpha)$ according to equation (3) is calculated by integrating

$$R(z, \alpha) = \frac{\int G(\nu, z, \alpha) F_{95}(\nu)\, {\rm d}\nu}{\int G(\nu, z, \alpha) F_{150}(\nu)\, {\rm d}\nu}, \quad (6)$$

where F_{95} and F_{150} are the measured filter response of the SPT 95 and 150 GHz bands, normalized such that the integral over each of the bands is 1. We have assumed the non-relativistic expression for $G(\nu, z, \alpha)$; however, we find that relativistic corrections have a negligible effect on our result. For the range of electron temperatures and optical depths expected in our cluster sample (e.g. Vikhlinin et al. 2009; Arnaud et al. 2010; Reichardt et al. 2013), including relativistic corrections from Itoh, Kohyama & Nozawa (1998) changes our final constraints on α by less than 1 per cent.

3 VERIFICATION OF METHOD WITH SIMULATIONS

We test the method described above using simulations. To do so, we make mock SPT observations of clusters that are formed in a large-volume, high-resolution cosmological hydrodynamical simulation (Dolag et al., in preparation). The simulation has been carried out with P-GADGET3, a modification of P-GADGET-2 (Springel 2005). The code uses an entropy-conserving formulation of SPH (Springel & Hernquist 2002) and includes treatment of radiative cooling, heating by a UV background, star formation and feedback processes from supernovae explosions and active galactic nuclei (Springel & Hernquist 2003; Fabjan et al. 2010). Cosmological parameters are chosen to match *WMAP*7 (Komatsu et al. 2011). The simulation box is 1244 Mpc per side and contains 1526^3 dark matter particles and as many gas particles, from which five simulated SZE light-cones, each of size $13^\circ \times 13^\circ$ (i.e. the total solid angle is 845 deg^2) have been extracted up to $z \sim 2$. From each of these simulated SZE maps, we then construct simulated SPT maps at 95 and 150 GHz.

The details of the construction of the simulated SZE light-cones will be presented in a forthcoming paper (Liu et al. 2014, in preparation), we highlight here the basic properties. In these mock observations, we include contributions from: (1) primary CMB anisotropies, (2) convolution with the SPT 150 and 95 GHz beams, (3) instrumental noise consistent with the observed SPT map depths of 18 and 44 μK arcmin for the 150 and 95 GHz bands, respectively, and (4) associated filter transfer functions for the two simulated bands. Finally, from these mock maps we identify clusters with the same approach adopted for real SPT clusters (e.g. Staniszewski et al.

2009; Reichardt et al. 2013), obtaining a sample of 212 clusters above signal to noise $\xi = 4.5$.

We then measure the ratio of the temperatures in the two bands, using the approach described in Section 2. We first convolve the 150 GHz maps to match the larger beam of the 95 GHz band. We then individually filter the 95 GHz and the 150 GHz maps with the 95 GHz filter and measure the signal at the position and θ_C scale that maximize the signal to noise in the multifrequency analysis. We then maximize the likelihood to determine α (equation 5). We recover $\alpha = 0.0019 \pm 0.022$, in agreement with the input value of $\alpha = 0$.

4 SPT RESULTS

We measure the temperature decrement ratios at the positions of the SPT-selected cluster sample from Reichardt et al. (2013), which included data from 720 of the 2500 deg^2 SPT-SZE survey. The SPT-SZE data used here has typical noise levels of 44 and 18 μK arcmin in CMB temperature units at 95 and 150 GHz, respectively. The exceptions are the two fields centred at 23^h30^m, -55° and 5^h30^m, -55° from Reichardt et al. (2013), which have a depth of 13 μK arcmin in the 150 GHz data used in this work. Since the publication of Reichardt et al. (2013), these fields had been re-observed in the SPT-SZE survey, with the new observations providing new 95 GHz measurements and deeper 150 GHz data. The final cluster sample used here consists of 158 clusters with both a $\xi > 4.5$ from Reichardt et al. (2013), and either a spectroscopic or photometric redshift reported in Song et al. (2012). We refer the reader to Staniszewski et al. (2009), Vanderlinde et al. (2010), Schaffer et al. (2011), Williamson et al. (2011) and Reichardt et al. (2013) for a detailed description of the survey strategy and data set characteristics.

We apply the same technique described in Section 2 and tested in Section 3 to measure the evolution of the CMB temperature with SPT clusters.

Using SPT data alone, we constrain the temperature evolution of the CMB to be

$$\alpha = 0.017^{+0.030}_{-0.028}, \quad (7)$$

which is consistent with the adiabatic expectation of $\alpha = 0$. We estimate the instrumental uncertainties associated with the beams, calibration and filter responses, and find them all to have a negligible result on this constraint. Moreover, the statistical uncertainty is ∼30 per cent larger than the limit on possible observational biases implied by the results of Section 3, implying that our analysis method is shown to be unbiased at or below the level of the statistical uncertainty.

We further combine our results with previously published data (Fig. 1). In particular, we include other cluster measurements (Luzzi et al. 2009; Hurier et al. 2014) and fine structure absorption lines (Noterdaeme et al. 2011; Muller et al. 2013). In doing this, we exclude from the likelihood calculation (equation 5) the 16 SPT clusters that were part of the main sample analysed by Hurier et al. (2014). We thus obtain a tighter constraint on the $T(z) = T_0(1 + z)^{(1-\alpha)}$ law:

$$\alpha = 0.005 \pm 0.012, \quad (8)$$

an ∼10 per cent improvement in measurement uncertainty in comparison to the previously reported $\alpha = 0.006 \pm 0.013$ (Hurier et al. 2014). We note that because the SPT data are on average a factor of 3 deeper than *Planck*, and the SPT beam is ∼8 times smaller, the SPT data set provides stronger constraints on a per cluster basis and is particularly well suited for studies of the high-redshift tail of the cluster distribution. In fact, only 4 per cent the *Planck*-selected clusters have redshifts larger than the median redshift of the SPT sample.

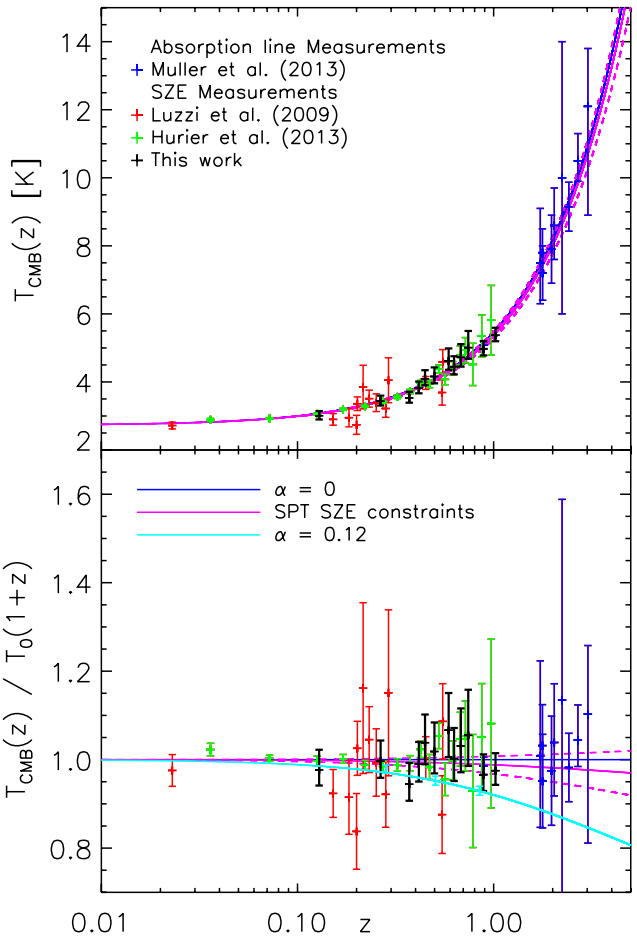

Figure 1. *Top panel:* measurements of the temperature of the CMB as a function of redshift. Blue points are absorption lines studies (see Muller et al 2013 and references therein). SZE measurements towards galaxy clusters are highlighted in red (see Luzzi et al. 2009 and references therein) and green for the stacked *Planck* SZE selected clusters (Hurier et al. 2014). Black points are the SPT-SZE cluster constraints. For visualization purposes, SPT clusters results have been obtained by reverting equation (1) from the measured constraints on α in each of 12 equally populated redshift bins. The blue continuous line corresponds to the relation $T(z) = T_0 \times (1 + z)$ and solid and dashed purple lines are the evolution corresponding to the best fit and $\pm 1\sigma$ models. *Bottom panel:* deviation of the measured temperature of the CMB as a function of redshift with respect to the adiabatic evolution. Cyan points represent the measured temperature of the CMB in three stacked redshift bins for a simulation with input value $\alpha = 0.12$ (cyan solid line).

The measurement presented here is consistent with the adiabatic evolution of the CMB radiation temperature ($\alpha = 0$) expected from the standard hot big bang model. Considering alternative cosmological models, Jetzer et al. (2011) demonstrated that measuring $T(z)$ at different redshifts allows one to constrain the effective equation of state of decaying dark energy ($p = w_{\rm eff}\rho$). Following Noterdaeme et al. (2011), by fitting the combined constraints on $T(z)$ with the temperature–redshift relation (equation 22 in Jetzer et al. 2011), taking $\Omega_{\rm m} = 0.255 \pm 0.016$ (Reichardt et al. 2013) and fixing the adiabatic index γ to the canonical value (4/3), we get

$w_{\rm eff} = -0.994 \pm 0.010$, which improves upon previous constraints (Noterdaeme et al. 2011; Hurier et al. 2014).

4.1 Selection bias

A number of possible selection biases could affect our measurements. In particular, cluster candidates were identified using a multiband matched-filter approach (Melin et al. 2006) where the temperature evolution of the Universe is assumed to be adiabatic. This could therefore bias our selection towards clusters that best mimic this behaviour. To show that this is not the case, we construct SPT mock light-cones similar to the ones presented in Section 3 but assuming different values of α. We then performed the same analysis described in Section 3 and show that we are able to recover the input value. Specifically, we test simulations with input values of α offset by more than 3σ from the adiabatic value, $\alpha = -0.12$ and 0.12. We then select clusters with the above described matched-filter multifrequency cluster finder under the assumption of adiabatic evolution and constrain α. We obtain unbiased measurements for the underlying input value $\alpha = -0.111^{+0.022}_{-0.018}$ and $\alpha = 0.110^{+0.014}_{-0.014}$, thus demonstrating that the selection is not driving our constraints (bottom panel of Fig. 1).

Another potential source of bias in our measurement of α is the fact that the temperature fluctuations of the CMB at the location of the SPT clusters should not average to zero. In fact, due to the adopted cluster selection, negative temperature fluctuations are more likely than positive ones (Vanderlinde et al. 2010). We estimate this effect to be negligible using the simulations described in Section 3. We also note that this effect should be less significant at larger SPT signal to noise ξ (Benson et al. 2013). If we restrict our analysis to the clusters with $\xi > 8$, which reduces the cluster sample by a factor of $\sim$6 to the 24 highest signal-to-noise clusters, we constrain $\alpha = 0.023^{+0.044}_{-0.038}$. This is consistent with our main result with only a modest 30 per cent increase in the uncertainty in α. This demonstrates that the constraints depend most significantly on the highest signal-to-noise clusters, which will be less biased by the CMB from the SPT selection. Similarly, we estimate the bias associated with lensed dusty sources to be unimportant for our analysis; their primary impact would be introducing some skewness in the scatter of clusters about our best-fitting model (Hezaveh et al. 2013).

Emission from cluster galaxies can also potentially bias our measurement. We estimate the effect to be negligible by performing the analysis presented here on subsamples of clusters above different ξ thresholds and by excluding clusters in proximity to known SUMSS sources (Mauch et al. 2003). All subsamples examined provide statistically consistent results. For example, using a subsample of 75 clusters with no associated SUMSS sources brighter than 20 mJy within a projected distance of 3 arcmin from the cluster centres, we obtain consistent results of $\alpha = 0.021^{+0.042}_{-0.038}$.

5 CONCLUSIONS

We have studied deviations from the adiabatic evolution of the mean temperature of the CMB in the form of $T(z) = T_0(1+z)^{(1-\alpha)}$. We present a method based on matched-filtering of clusters at the SPT frequencies and show that we are able to recover unbiased results using simulated clusters. The simulated light-cones we use come from a large cosmological hydrodynamical simulation and include realistic SPT beam effects, CMB anisotropy and SPT noise levels for both the 150 and 95 GHz bands.

We apply this method to a sample of 158 SPT clusters selected from 720 square degrees of the 2500 square degree SPT-SZE survey, which span the redshift range $0.05 < z < 1.35$, and measure $\alpha = 0.017^{+0.030}_{-0.028}$, consistent with the standard model prediction of $\alpha = 0$. Our measurement gives competitive constraints and significantly extends the redshift range with respect to previously published results based on galaxy clusters (e.g. Luzzi et al. 2009; Avgoustidis et al. 2012; de Martino et al. 2012; Muller et al. 2013; Hurier et al. 2014). Combining our measurements with published data, we obtain $\alpha = 0.005 \pm 0.012$, improving current published constraints.

Such tight limits on deviations from the adiabatic evolution of the CMB also put interesting constraints on the effective equation of state of decaying dark energy models, $w_{\rm eff}$. Indeed, from SPT clusters alone we are able to measure $w_{\rm eff} = -0.988^{+0.029}_{-0.033}$, in good agreement with previous constraints based on quasar absorption lines (Noterdaeme et al. 2011) and other SZE measurements from clusters (Hurier et al. 2014).

Future analyses will be able to draw upon larger cluster samples (e.g. the full 2500 square degree SPT-SZE survey and the upcoming SPTpol and SPT-3G surveys) and quasar surveys (e.g. SDSS III). By expanding the data volume at high redshifts, these surveys will enable precision tests of the temperature evolution of the CMB across cosmic time. Moreover, because clusters and quasars suffer from different systematics, the comparison will provide an important cross-check on systematics. These surveys will improve constraints on non-standard cosmological models.

ACKNOWLEDGEMENTS

The Munich SPT group is supported by the DFG through TR33 'The Dark Universe' and the Cluster of Excellence 'Origin and Structure of the Universe'. The South Pole Telescope programme is supported by the National Science Foundation through grant ANT-0638937. Partial support is also provided by the NSF Physics Frontier Center grant PHY-0114422 to the Kavli Institute of Cosmological Physics at the University of Chicago, by the Kavli Foundation and the Gordon and Betty Moore Foundation and by NASA grant number PF2-130094. Galaxy cluster research at Harvard is supported by NSF grants AST-1009012 and DGE-1144152. Galaxy cluster research at SAO is supported in part by NSF grants AST-1009649 and MRI-0723073. The McGill group acknowledges funding from the National Sciences and Engineering Research Council of Canada, Canada Research Chairs programme, and the Canadian Institute for Advanced Research.

REFERENCES

Arnaud M., Pratt G. W., Piffaretti R., Böhringer H., Croston J. H., Pointecouteau E., 2010, A&A, 517, A92
Avgoustidis A., Luzzi G., Martins C. J. A. P., Monteiro A. M. R. V. L., 2012, J. Cosmol. Astropart. Phys., 2, 13
Battistelli E. S. et al., 2002, ApJ, 580, L101
Benson B. A. et al., 2013, ApJ, 763, 147
Carlstrom J. E. et al., 2011, PASP, 123, 568
Cavaliere A., Fusco-Femiano R., 1976, A&A, 49, 137
de Martino I., Atrio-Barandela F., da Silva A., Ebeling H., Kashlinsky A., Kocevski D., Martins C. J. A. P., 2012, ApJ, 757, 144
Fabbri R., Melchiorri F., Natale V., 1978, Ap&SS, 59, 223
Fabjan D., Borgani S., Tornatore L., Saro A., Murante G., Dolag K., 2010, MNRAS, 401, 1670
Fixsen D. J., 2009, ApJ, 707, 916
Hezaveh Y., Vanderlinde K., Holder G., de Haan T., 2013, ApJ, 772, 121

Hurier G., Aghanim N., Douspis M., Pointecouteau E., 2014, A&A, 561, A143
Itoh N., Kohyama Y., Nozawa S., 1998, ApJ, 502, 7
Jaeckel J., Ringwald A., 2010, Ann. Rev. Nucl. Part. Sci., 60, 405
Jetzer P., Tortora C., 2011, Phys. Rev. D, 84, 043517
Jetzer P., Puy D., Signore M., Tortora C., 2011, Gen. Relativ. Gravit., 43, 1083
Komatsu E. et al., 2011, ApJS, 192, 18
Lima J. A. S., Silva A. I., Viegas S. M., 2000, MNRAS, 312, 747
Luzzi G., Shimon M., Lamagna L., Rephaeli Y., De Petris M., Conte A., De Gregori S., Battistelli E. S., 2009, ApJ, 705, 1122
Martins C. J. A. P., 2002, Phil. Trans. R. Soc. A, 360, 2681
Matyjasek J., 1995, Phys. Rev. D, 51, 4154
Mauch T., Murphy T., Buttery H. J., Curran J., Hunstead R. W., Piestrzynski B., Robertson J. G., Sadler E. M., 2003, MNRAS, 342, 1117
Melin J.-B., Bartlett J. G., Delabrouille J., 2006, A&A, 459, 341
Molaro P., Levshakov S. A., Dessauges-Zavadsky M., D'Odorico S., 2002, A&A, 381, L64
Muller S. et al., 2013, A&A, 551, A109
Murphy M. T., Webb J. K., Flambaum V. V., 2003, MNRAS, 345, 609
Nagai D., Kravtsov A. V., Vikhlinin A., 2007, ApJ, 668, 1
Noterdaeme P., Petitjean P., Srianand R., Ledoux C., López S., 2011, A&A, 526, L7
Overduin J. M., Cooperstock F. I., 1998, Phys. Rev. D, 58, 043506
Planck Collaboration, 2013, preprint (arXiv:1303.5080)
Puy D., 2004, A&A, 422, 1
Reichardt C. L. et al., 2013, ApJ, 763, 127
Rephaeli Y., 1980, ApJ, 241, 858
Schaffer K. K. et al., 2011, ApJ, 743, 90
Song J. et al., 2012, ApJ, 761, 22
Springel V., 2005, MNRAS, 364, 1105
Springel V., Hernquist L., 2002, MNRAS, 333, 649
Springel V., Hernquist L., 2003, MNRAS, 339, 289
Srianand R., Petitjean P., Ledoux C., 2000, Nature, 408, 931
Srianand R., Chand H., Petitjean P., Aracil B., 2004, Phys. Rev. Lett., 92, 121302
Srianand R., Noterdaeme P., Ledoux C., Petitjean P., 2008, A&A, 482, L39
Staniszewski Z. et al., 2009, ApJ, 701, 32
Sunyaev R. A., Zel'dovich Y. B., 1972, Comments Astrophys. Space Phys., 4, 173
Sunyaev R. A., Zeldovich Y. B., 1980, MNRAS, 190, 413
Tolman R. C., 1934, Relativity, Thermodynamics and Cosmology. The Clarendon Press, Oxford
Vanderlinde K. et al., 2010, ApJ, 722, 1180
Vikhlinin A. et al., 2009, ApJ, 692, 1033
Williamson R. et al., 2011, ApJ, 738, 139

[1]*Department of Physics, Ludwig-Maximilians-Universität, Scheinerstr. 1, D-81679 München, Germany*
[2]*Excellence Cluster Universe, Boltzmannstr. 2, D-85748 Garching, Germany*
[3]*Max-Planck-Institut für extraterrestrische Physik, Giessenbachstr. D-85748 Garching, Germany*
[4]*University of Chicago, 5640 South Ellis Avenue, Chicago, IL 60637, USA*
[5]*Harvard–Smithsonian Center for Astrophysics, 60 Garden Street, Cambridge, MA 02138, USA*
[6]*Department of Physics, Harvard University, 17 Oxford Street, Cambridge, MA 02138, USA*
[7]*Center for Particle Astrophysics, Fermi National Accelerator Laboratory, Batavia, IL 60510, USA*
[8]*Kavli Institute for Cosmological Physics, University of Chicago, 5640 South Ellis Avenue, Chicago, IL 60637, USA*
[9]*Enrico Fermi Institute, University of Chicago, 5640 South Ellis Avenue, Chicago, IL 60637, USA*
[10]*Department of Physics, University of Chicago, 5640 South Ellis Avenue, Chicago, IL 60637, USA*
[11]*Argonne National Laboratory, 9700 S. Cass Avenue, Argonne, IL 60439, USA*
[12]*Department of Physics and Astronomy, University of Missouri, 5110 Rockhill Road, Kansas City, MO 64110, USA*
[13]*Department of Astronomy and Astrophysics, University of Chicago, 5640 South Ellis Avenue, Chicago, IL 60637, USA*
[14]*NIST Quantum Devices Group, 325 Broadway Mailcode 817.03, Boulder, CO 80305, USA*
[15]*Instituto de Astrofísica Pontificia Universidad Católica de Chile Vicuña Mackenna 4860, 7820436 Macul Santiago, Chile*
[16]*Department of Physics, McGill University, 3600 Rue University, Montreal, QC H3A 2T8, Canada*
[17]*Astronomy Department, University of Illinois at Urbana-Champaign, 1002 W. Green Street, Urbana, IL 61801, USA*
[18]*Department of Physics, University of Illinois Urbana-Champaign, 1110 W. Green Street, Urbana, IL 61801, USA*
[19]*Department of Physics, University of California, Berkeley, CA 94720, USA*
[20]*Department of Astronomy, University of Florida, Gainesville, FL 32611, USA*
[21]*Department of Astrophysical and Planetary Sciences and Department of Physics, University of Colorado, Boulder, CO 80309, USA*
[22]*Kavli Institute for Particle Astrophysics and Cosmology, Stanford University, 452 Lomita Mall, Stanford, CA 94305-4085, USA*
[23]*Department of Physics, Stanford University, 452 Lomita Mall, Stanford, CA 94305-4085, USA*
[24]*Physics Division, Lawrence Berkeley National Laboratory, Berkeley, CA 94720, USA*
[25]*California Institute of Technology, 1200 E. California Blvd, Pasadena, CA 91125, USA*
[26]*Steward Observatory, University of Arizona, 933 North Cherry Avenue, Tucson, AZ 85721, USA*
[27]*Kavli Institute for Astrophysics and Space Research, Massachusetts Institute of Technology, 77 Massachusetts Avenue, Cambridge, MA 02139, USA*
[28]*Department of Physics, University of Michigan, 450 Church Street, Ann Arbor, MI 48109, USA*
[29]*Physics Department, Center for Education and Research in Cosmology and Astrophysics, Case Western Reserve University, Cleveland, OH 44106, USA*
[30]*Physics Department, University of Minnesota, 116 Church Street S.E., Minneapolis, MN 55455, USA*
[31]*Space Telescope Science Institute, 3700 San Martin Dr., Baltimore, MD 21218, USA*
[32]*Liberal Arts Department, School of the Art Institute of Chicago, 112 S Michigan Ave, Chicago, IL 60603, USA*
[33]*Dunlap Institute for Astronomy & Astrophysics, University of Toronto, 50 St George St, Toronto, ON M5S 3H4, Canada*
[34]*Department of Astronomy & Astrophysics, University of Toronto, 50 St George St, Toronto, ON M5S 3H4, Canada*

This paper has been typeset from a TEX/LATEX file prepared by the author.